



HAL
open science

An Optimized Buffer for Repeatable Multicolor STORM

Vaky Abdelsayed, Hadjer Boukhatem, Nicolas Olivier

► **To cite this version:**

Vaky Abdelsayed, Hadjer Boukhatem, Nicolas Olivier. An Optimized Buffer for Repeatable Multicolor STORM. ACS photonics, In press, 10.1021/acsp Photonics.2c01249 . hal-03871254

HAL Id: hal-03871254

<https://hal.science/hal-03871254>

Submitted on 25 Nov 2022

HAL is a multi-disciplinary open access archive for the deposit and dissemination of scientific research documents, whether they are published or not. The documents may come from teaching and research institutions in France or abroad, or from public or private research centers.

L'archive ouverte pluridisciplinaire **HAL**, est destinée au dépôt et à la diffusion de documents scientifiques de niveau recherche, publiés ou non, émanant des établissements d'enseignement et de recherche français ou étrangers, des laboratoires publics ou privés.

An Optimized Buffer for Repeatable Multicolor STORM

Vaky Abdelsayed, Hadjer Boukhatem, and Nicolas Olivier*

*Laboratory for Optics and Biosciences (LOB), CNRS, INSERM, École Polytechnique, IP Paris,
91128 Palaiseau, France*

E-mail: nicolas.olivier@polytechnique.edu

Abstract

Stochastic Optical Reconstruction Microscopy (STORM) is a popular method of super-resolution microscopy, due to moderate requirements on the optical setup, and high achievable resolution. However, since its inception more than 15 years ago, protocols have barely evolved, and despite some recent progress, multicolor imaging can still be complex without the right equipment. To achieve better multicolor images, we decided to optimize the buffer composition to improve the blinking of the most popular red dye CF-568 while maintaining good performance for far-red fluorophores such as Alexa-647 using four optimization parameters, namely the concentration of three chemicals and the pH. We developed a simple, inexpensive and stable buffer, that can be stored several weeks and frozen for longer term storage that allow high quality 3-color STORM imaging.

Keywords

Microscopy, Fluorescence, Single-molecule, Super-resolution, Optical imaging, Photoswitching

Introduction

STORM microscopy¹ is a powerful optical super-resolution method, that can now yield sub-10 nm resolution in 3D for multiple colors on optimized optical setups.² The key to this method is to induce reversible switching of (mainly organic) fluorophores by controlling their chemical environment.³⁻⁵ Most studies still rely on the original chemical environment - a combination of enzymatic oxygen scavengers (usually, Glucose-oxydase and catalase) and a reducing thiol such as 2-Mercaptoethylamine/Cysteamine (MEA) or β -Mercaptoethanol (β ME) - as the blinking mechanism of the most popular fluorophores Cy5/Alexa-647 has been well-studied in this environment.⁶ Moreover, several screens have identified dyes that perform well in this buffer,^{7,8} with the most promising 2-color combination being CF-568 and Alexa-647. Far-red fluorophores excited at \approx 750 nm have also been used^{7,9} with success in combination with Alexa-647, but unfortunately most commercial microscopes do not offer this laser wavelength. Further, lower photon counts for 750-nm excited dyes than for Alexa-647 means the buffers have to be optimized specifically to obtain comparable resolution in both channels.^{9,10} Another popular multicolor solution relies on simultaneous excitation of 640-nm excited dyes followed by spectral un-mixing,^{8,11,12} which can be used for up to 3 colors simultaneously, but requires specific analysis software which only recently became publicly available^{13,14} and has limitations in terms of cross-talk for dense regions and for the identification of structures of interest.

In order to improve multicolor STORM imaging protocols, we decided to focus on CF-568, the most popular second color for STORM, and to optimize the buffers by quantifying the image quality of microtubules samples (see Methods). This approach does not provide photophysical parameters such as off-times or absolute numbers of blinking events (as they can be measured once the optimization has been performed) but does provide enough quantitative measure of image quality to perform the optimization. In terms of parameters to optimize for the buffer composition, we made the following decisions:

(1) To use Sodium Sulfite as an oxygen scavenger.¹⁵ It is simple to use compared to enzymatic

systems, reduces costs, and provides stability (both temporal, and in terms of pH).(see Supporting Text 1 for a discussion on the different oxygen scavenging options)

(2) To use DTT as the primary reducing agent. It can be purchased as a 1 M solution, so does not have to be prepared fresh from a powder as MEA, and is not as stinky nor as toxic as β ME.

(3) To use DABCO¹⁶ as an additional triplet-state quencher. DABCO was previously used to improve the blinking of Cy3 in Vectashield¹⁷ and does not prevent the blinking of Alexa-647 when added to the canonical buffer.¹⁸

(4) To vary the pH, that is known to affects the blinking of dyes¹⁹⁻²¹, which is made simple by the use of Sodium Sulfite that does not lead to acidification and the possibility to prepare large volumes of buffers to accurately measure pH using pH-meter.

(5) To use water as the main solvent. While higher index media are very useful for 3D imaging^{15,17,22} they make TIRF imaging more difficult, and the majority of STORM imaging is performed in TIRF or grazing incidence²³ with TIRF-based z-stabilization.

We also decided to work on a fairly simple microscope (see Methods and Figure S1: epillumination using multimode lasers and fibers, multicolor dichroic and filters), and not to use any UV reactivation to make sure the protocols are generally applicable.

Methods

Optical setup

Buffer optimization for CF-568 was performed on a home built microscope (see Fig S1) based on the MiCube design,²⁴ equipped with an Olympus 100x 1.45NA objective, and a 200 mm infinity-corrected tube lens (Thorlabs ITL200), resulting in 111 \times magnification on the camera (Andor iXon), for an effective pixel size of 144 nm. The sample was placed on a 300 μ m range z-piezo stage (LTZ-300, Piezoconcept) with manual lateral movement which is the only moving part of the system. We used a 5 color dichroic mirror and emission filter (Semrock FF409/493/573/652/759-Di01 + FF01-432/515/595/681/809), and added an additional filter to remove laser reflections

(ET605/70m (Chroma) for CF-568). We used a 561 nm laser (100 mW, Cobolt) coupled to a 400 μm Multi-Mode fiber (M28L02, Thorlabs) which was shaken using a fan to cancel out speckles, and the intensity at the sample from the 561 nm laser used for the buffer optimization was in the 1-3 kW/cm^2 range. We decided to qualitatively optimize the laser power²⁵ for each buffer condition (by changing the laser power on a cell and visually optimizing the blinking before recording a dataset on another cell) since we thought using the same laser power every time could lead us to a local maximum.

Further imaging including 2-color and 3-color STORM was performed on an IX83 Inverted microscope (Olympus) using a 100x 1.3NA objective (Olympus) and an Orca Fusion sCMOS camera (Hamamatsu) using the slowest read-out speed. We used a single mode 532 nm laser (Voltran, 40 mW), a single mode 561 nm laser (100 mW, Cobolt), a 635 nm multimode laser (700 mW, Lasertak) and a 750 nm multimode laser (1.2 W Oxxius), the later 3 were coupled into a 400 μm Multi-Mode fiber (M28L02, Thorlabs) which was shaken with a fan as shown in Figure S1. The microscope is equipped with Chroma filters: 532 nm and 640 nm-excited fluorophores were imaged using a ZT532/640rpc 2-color dichroic mirror and a ET605/70 or ET700-75 emission filter. Due to the double-deck design, the emitted light also goes through a T550lpxr or a T660lpxr dichroic mirror. 750 nm-excited fluorophores were imaged using a T760lpxr dichroic mirror and a ET810-90 emission filter. Similarly, the emitted light also goes through an additional T760lpxr dichroic mirror.

Sample preparation and immunofluorescence staining

African green monkey kidney cells (COS-7) were cultured in DMEM-Glutamax (Gibco 10566016) supplemented with 10% FBS in a cell culture incubator (37°C and 5% CO₂). Cells were plated at low confluency on ethanol-cleaned 25 mm #1.5 thickness round coverglass (VWR) for imaging. Prior to fixation, all solutions were pre-warmed to 37°C. 24h after plating, cells were pre-extracted for 30 s in 0.25% Triton X-100 (Sigma-Aldrich) in PHEM (60 mM PIPES, 25 mM HEPES, 10 mM EGTA, 4 mM MgSO₄), washed once in PHEM, fixed for 8 min in -20°C Methanol (Sigma-

Aldrich), then washed 3 times with PBS. The samples were then blocked for 1h in 5% BSA, before being incubated for 1.5h at room temperature with 1:500 rat anti alpha-tubulin antibodies (abcam ab6160) in 1% BSA diluted in PBS-0.2% Triton (BSA-PBST), followed by 3 washes with PBST, and then incubated for 1h in BSA-PBST with a goat anti-rat CF-568 (Sigma SAb4600086) secondary antibodies, 1:500

For further imaging after the optimization was performed and for multicolor imaging, we used glutaraldehyde fixation based on the the protocol from,²⁶ with a pre-extraction step of 30 seconds in PHEM-0.25% Triton + 0.1% glutaraldehyde, followed by fixation in PHEM-0.25% Triton + 0.5% glutaraldehyde for 8 minutes, and quenching in PBS-0.1% NABH4 for 8 minutes and finally 3 washes in PBS. The samples were then blocked for 1h in 5% BSA, before performing the immunostaining. We incubated the primary antibodies for 1.5h in BSA-PBST at room temperature followed by 3 washes with PBST and incubation with secondary antibodies for 1h in BSA-PBST. For single color imaging, we use two different primary antibodies: mouse anti alpha-tubulin (Sigma T6199) 1:500 and rat anti alpha-tubulin (abcam ab6160) 1:500, with the following secondary antibodies: (Fig 2,3) Goat anti-rat CF 568 (Sigma SAb4600086) 1:500, (Fig 4) Goat anti-rat Alexa Fluor 647 (Invitrogen A21247) 1:500 Horse anti-mouse Dylight 649 (Vectorlab DI-2649) 1:500, Goat anti-mouse CF 647 (Sigma SAb4600182) 1:500, (Fig 5) Goat anti-mouse CF 750 (Sigma SAb4600211) 1:250, Donkey anti-rat Dylight 755 (Invitrogen SA510031) 1:250, and Goat anti-rat CF 770 (Sigma SAb4600479) 1:250.

For 2-color imaging (Figure 6), we used Mouse anti alpha-tubulin (Sigma T6199) 1:500 and Rabbit anti clathrin heavy chain (abcam, ab21679) 1:500, and for secondaries Goat anti-mouse CF 647 (Sigma SAb4600182) 1:500 and Donkey anti-rabbit CF 568 (Sigma, SAB4600076) 1:500.

For 3-color imaging (Figure 7), we used Mouse anti alpha-tubulin (Sigma T6199) 1:500 and Rabbit anti clathrin heavy chain (abcam, ab21679) 1:500, and for secondaries goat anti-mouse CF 750 1:250 (Sigma SAb4600211) and Donkey anti-rabbit CF 568 1:500 (Sigma, SAB4600076). We finally added Alexa Fluor 647 Phalloidin (Thermofisher A22287) 1:200 one hour in PBS just before imaging, and rinsed twice in PBS.

The sample were imaged in an Attofluor imaging chamber (Invitrogen, A7816), with 1 ml of imaging buffer and another 25 mm round coverglass on top to limit air exchanges.

Buffer preparation

- DABCO [1,4-di-azobicyclo-(2.2.2.)-octane] (D27802, Sigma) was dissolved in distilled water to make a 1 M stock solution, adding HCl 12 M until all the powder was dissolved and the pH reached pH 8.0. The pH value is critical since it mostly determines the pH of the overall buffer. The stock solution was kept in the fridge in the dark for several weeks.

- DTT 1 M (43816, Sigma) was used directly as purchased and was kept in the fridge for several weeks.

- Sodium Sulfito (S0505, Sigma) was dissolved in PBS 10x to 1 M as in,¹⁵ and was kept at room temperature on the bench for several weeks.

We typically prepared 10 mL of buffer at a time, and we adjusted the pH using NaOH and HCl and a pH-meter (Mettler Toledo FE20) and stored it in the fridge. The composition of all buffer conditions tested in this paper is given in Table S1.

Data acquisition

For the buffer optimization of CF-568, we acquired 12,000 images with ≈ 50 ms integration time using the conventional amplifier of the EMCCD camera, did not add UV light (which limits the achievable density, but makes comparing conditions easier), and manually corrected z-drift. The camera and z-piezo were controlled using micro-manager.²⁷ 561 nm laser power at the sample was typically between 1 and 2 kW/cm^2

For further imaging with the optimized buffer, we acquired between 10,000 and 30,000 images using micro-manager, using active z-stabilization on the IX83 except at 750 nm since the dichroic used for focus stabilization prevents the transmission of the fluorescent signal. Laser power at 532 nm, 561 nm, 640 nm and 750 nm was typically between 1 and 4 kW/cm^2 .

Data processing

Raw STORM image stacks were processed using a FIJI macro that runs an analysis with Detection of Molecules (DoM)²⁸ and Thunderstorm,²⁹ including drift-correction and grouping of consecutive localizations. Using a python script, the distributions of SNR and number of photons obtained using the manufacturer's count-to-photon conversion factor, as well as the density of fluorophores, were averaged. SNR and photon counts are expected to be highly correlated measurements, but we kept both since discrepancies between the two metrics can help us identify conditions with poor blinking that can affect one of the two measurements. To calculate the density of fluorophores, the STORM image was divided in small bins of 30 nm \times 30 nm, and the number of molecules in the image was divided by the total surface area of the bins occupied by at least one fluorophore. (The two scripts are available on github³⁰). Fourier Ring Correlation (FRC)³¹ values shown in figure 2 and 3 were calculated using the BIOP FIJI plugin³² with DoM localizations exported in Thunderstorm format to create two images with 5 nm pixels using localizations from odd and even frames respectively. This script, modified from^{33,34} is also available on github.³⁰ The diffraction limited images shown in figure 2 and 3 are the standard deviation of the raw STORM data, computed using FIJI. See Figure S3 for the other FRC value given in figures 4-7.

Results

Optimization of CF-568 blinking

We first started with a buffer composition of 30 mM Sodium Sulfite and 30 mM DTT, which is close to what was demonstrated to work with Alexa-647 with MEA instead of DTT,¹⁵ and looked at the influence of both pH and DABCO concentration. The mean SNR, photon count and density of molecules per dataset were studied using 11 buffers within a pH range of 7-9 and a concentration range of 0-150 mM for DABCO (figure 1-a1,b1 & c1). A maximal point was reached for the three parameters for the buffer with a pH value 7.7 and DABCO concentration 65 mM. This pH value

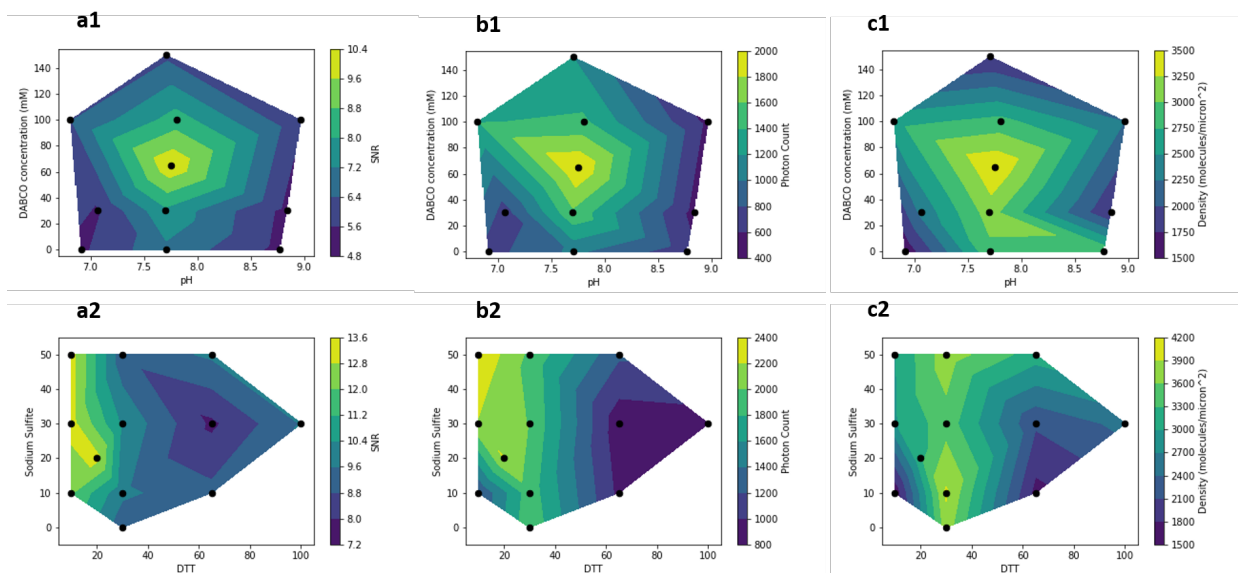


Figure 1: Interpolated plots for SNR, density and photon count of CF-568 as a function of the buffer composition for the 22 buffers tested for the first round of optimization. Experimental measurements correspond to the dark spots. (a1) SNR (b1) Photon counts and (c1) molecular density for 11 buffers with sodium sulfite concentration of 30 mM, DTT concentration of 30 mM, pH value given on the x-axis, and DABCO concentration on the y-axis. (a2) SNR (b2) Photon counts and (c2) molecular density for 12 buffers with DABCO concentration of 30 mM, a pH of 7.7, DTT concentration given on the x-axis, and sodium sulfite concentration on the y-axis.

of 7.7 agrees with the optimal value of 7.5 found for STORM imaging of Alexa-647 when using DTT as a reducing agent.¹⁸

We then fixed the pH to a value around 7.7 and the DABCO concentration to 65 mM and studied the influence of DTT and sodium sulfite concentrations by preparing 12 buffers with a concentration range of 10-100 mM for DTT and 0-50 mM for sodium sulfite (figure 1-a2,b2 & c2). The photon count and the density were highest for buffers with DTT concentration between 20 and 30 mM except when the sodium sulfite concentration was less than 10 mM. The buffers with 10 mM of DTT and 30 or 50 mM sodium sulfite also showed high SNR values but were not further considered since they displayed lower molecular density (Fig 1-c2), and high level of discontinuity was observed by visual check in the final images. Hence, the optimal range was found for buffers with a DTT concentration around 20-30 mM and having a sodium sulfite concentration above 10 mM.

To make sure we indeed reached an optimum for the chemical conditions of our buffer, we changed again the pH and DABCO concentration for a fixed DTT and sodium sulfite concentrations of 20 mM. We first set the DABCO concentration to 65 mM. Testing 3 buffers having respective pH values around 7, 8 and 9 clearly showed better results for the buffer with pH 8 (See Figure S2). In a similar manner, starting from 2 conditions, one with concentrations of DTT and sodium sulfite of 20 mM, the other with DTT concentration of 30 mM and a sodium sulfite concentration of 10 mM, we set the pH to 8 and we prepared 4 buffers with DABCO concentration in the range 0-100 mM. In both cases, we found values quite comparable to those obtained with 30 mM DTT and 30 mM Sulfite (See Figure S2) so decided further optimization was unnecessary and set the buffer conditions to DTT 30 mM, sodium sulfite 30 mM, DABCO 65 mM, with a pH value of 8 for further studies.

We then tested this protocol on another microscope equipped with an active stabilization system and a single mode laser excitation at 532 nm (see Methods). We once again imaged microtubules, and obtained convincing results. As can be seen in Figure 2 (a), the raw images show bright isolated molecules, and imaging can be performed for a long enough time to achieve a high density of molecules, resulting in a STORM image (Figure 2 c) with a much better resolution than the diffraction-limited image reconstructed from the same dataset (Figure 2 b). To estimate the resolution of our image, we performed a FRC³¹ calculation which yielded a resolution of 11.5 nm. We then performed some further quantification to provide a more complete picture of the photo-physics of the dye in this buffer by characterizing ON-times, duty cycle, bleaching fraction, and mean number of blinks from the signal of isolated antibodies (see Figure S4). Photon counts are much higher than those measured in the optimization process (mean value of ≈ 5600 compared to ≈ 2200), which is due to the combination of a better microscope and a different camera. Convinced that our imaging protocol worked well enough to do high quality STORM imaging, we decided to test how stable our buffer was.

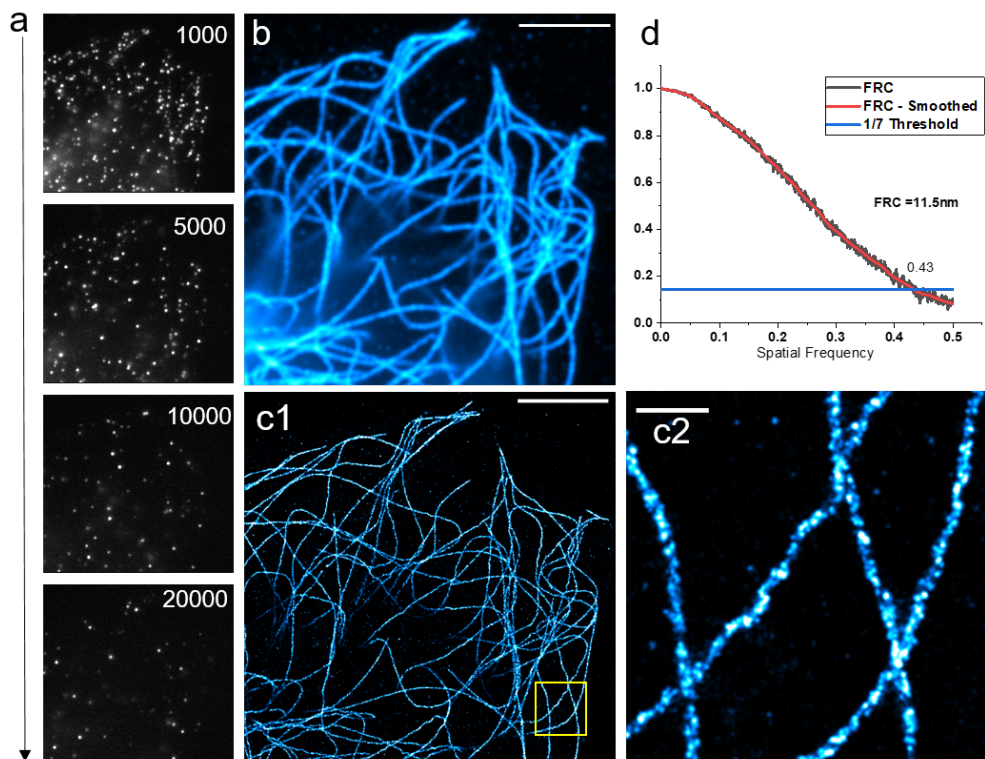


Figure 2: α -tubulin stained with CF-568 in our optimized buffer. (a) Raw camera frames with frame number indicated in the top-right corner (b) diffraction limited image (c) STORM image, reconstructed from ≈ 1.4 million molecules localizations in 26,000 frames. Scalebar: $5\mu\text{m}$, 500 nm in inset. (d) FRC curve for the dataset, giving an FRC resolution of 11.5 nm

Testing the long-term stability of the buffer

We froze 10 mL of our optimized buffer and left it at -20°C for a week. We then left it overnight in the fridge to thaw and performed imaging the next day, as well as 4 days later (keeping the buffer in the fridge once thawed). We noticed no strong changes in the performance of the buffer (See Figure 3) enabling the preparation of a large batch of buffer followed by aliquoting and freezing, guaranteeing reproducible performances throughout a STORM imaging project.

Testing 640 nm excited fluorophores in the optimized buffer

Our initial assumption was that the ingredients of the buffer were chosen to insure good blinking of Alexa-647, but we had to confirm this. We therefore immunostained α -tubulin once again,

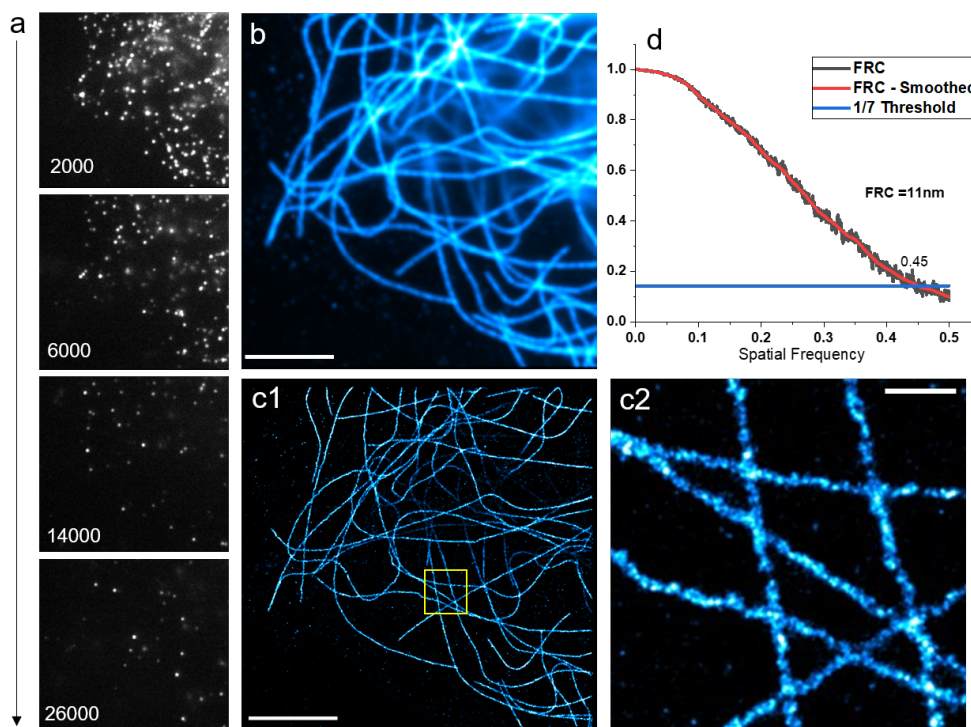


Figure 3: α -tubulin stained with CF-568 in our optimized buffer after freezing 1 week and thawing overnight in the fridge and waiting 4 days (a) Raw camera frames with frame number indicated in the bottom-right corner (b) diffraction limited image (c) STORM image, reconstructed from ≈ 1.1 million molecules localizations in 30,000 frames. Scalebar: $5\mu\text{m}$, 500 nm in inset. (d) FRC curve for the dataset, giving an FRC resolution of 11 nm

and tested 3 popular far-red dyes, Alexa-647, Dylight-649 and CF-647, and obtained high quality images for all three with FRC resolutions in the 20-30 nm range, in line with values published in the literature with other buffers^{21,25} as shown in Figure 4 and in Figure S3.

We quantified the average photon counts and density of molecules for all three dyes in our buffer, and the values are given in Table 1. As with CF-568, we also used the fluorescent signal from isolated antibodies to provide a more complete description of the blinking of the fluorophores (duty cycle, ON-time, bleaching fraction...) in this buffer in Figures S5-7. All three dyes display high photon number, as well as high molecular density resulting in high quality images. We did notice however that in this wavelength range, two populations of molecules seemed to co-exist, as we could see on the raw data some bright short-lived molecules as well as some dim longer-lived ones (See Figure S7D).

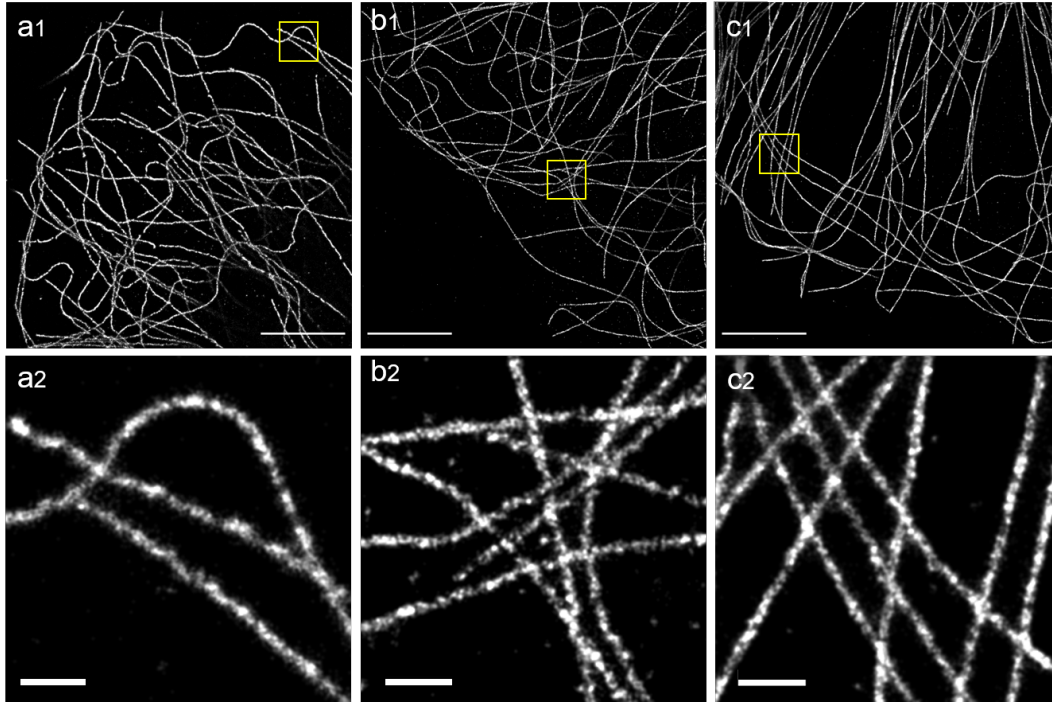


Figure 4: Test of several 640nm-excited fluorophores on α -tubulin . (a) Alexa-647 [FRC resolution: 33 nm] (b) Dylight-649 [FRC resolution: 32 nm] and (c) CF-647 [FRC resolution: 22 nm]. Scalebars: $5\mu\text{ m}$, 500 nm in inset

Table 1: Comparison between the three different red dyes tested. The density is in molecules per μm^2 excluding empty pixels. (see Methods)

Dye	Photon count	Density
Alexa-647	5793	6367
CF-647	5976	5716
Dylight-649	7640	5091

Testing 750 nm excited fluorophores in the optimized buffer

Having made sure the usual 640 nm excited fluorophores worked, we tested several 750 nm excited dyes. These dyes have generally been shown to blink well with 640 nm excited fluorophores,⁷ but provide fairly low photon counts. We tested 3 dyes: Dylight 755, CF-750 and CF-770. In all 3 cases, we could reconstruct good quality images, as can be seen in figure 5 but the photon counts and FRC values were as expected lower than for the other 2 colors (see Table 2 and Figure S3). As with the other fluorophores, we provide a more complete description of the blinking of the fluorophores (duty cycle, ON-time, bleaching fraction, mean number of blinks...) in this buffer in

Figures S8-10.

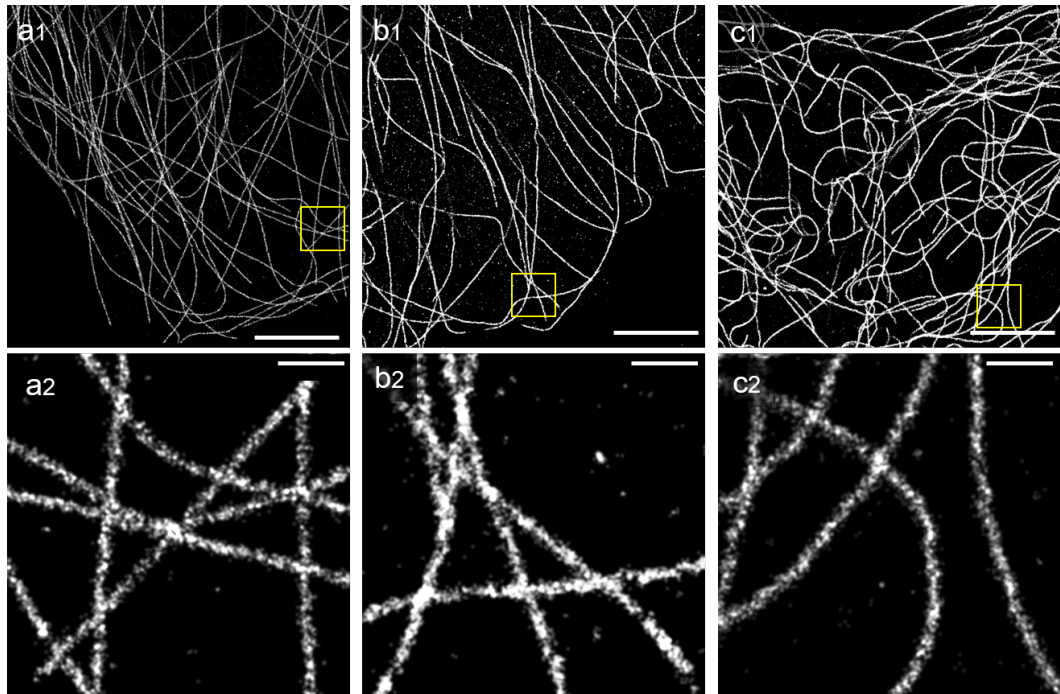


Figure 5: Test of several 750 nm-excited fluorophores on α -tubulin . (a) CF-750 [FRC resolution: 50 nm] (b) Dylight-755 [FRC resolution: 24 nm] and (c) CF-770 [FRC resolution: 65 nm]. Scale-bars: $5\mu\text{m}$, 500 nm in inset.

Table 2: Comparison between the three different far-red dyes tested. The density is in molecules per μm^2 excluding empty pixels

Dye	Photon count	Density
CF-750	1647	2402
Dylight-755	2900	2470
CF-770	2100	2620

We then tested whether the low photon counts of 750 nm excited dyes could be increased by adding COT for imaging CF-750, as in,^{9,10} and could indeed notice a marked improvement in both photon counts and FRC resolution. (See Figure S11.)

Multicolor imaging

Having just demonstrated that the far-red fluorophores tested worked well in our buffer, we decided to perform some multicolor STORM imaging.

2-color imaging

The most common laser combination on STORM microscopes is 532 nm and 640 nm, so we first tested how well our buffer behaved for a typical 2-color experiment, and chose the popular combination of microtubules (α -tubulin) and clathrin.³⁵ We stained microtubules with CF-647, and clathrin with CF-568, and imaged the two dyes sequentially starting with CF-647. Figure 6 shows images comparable to that obtained with a single fluorophore, demonstrating negligible cross talk.

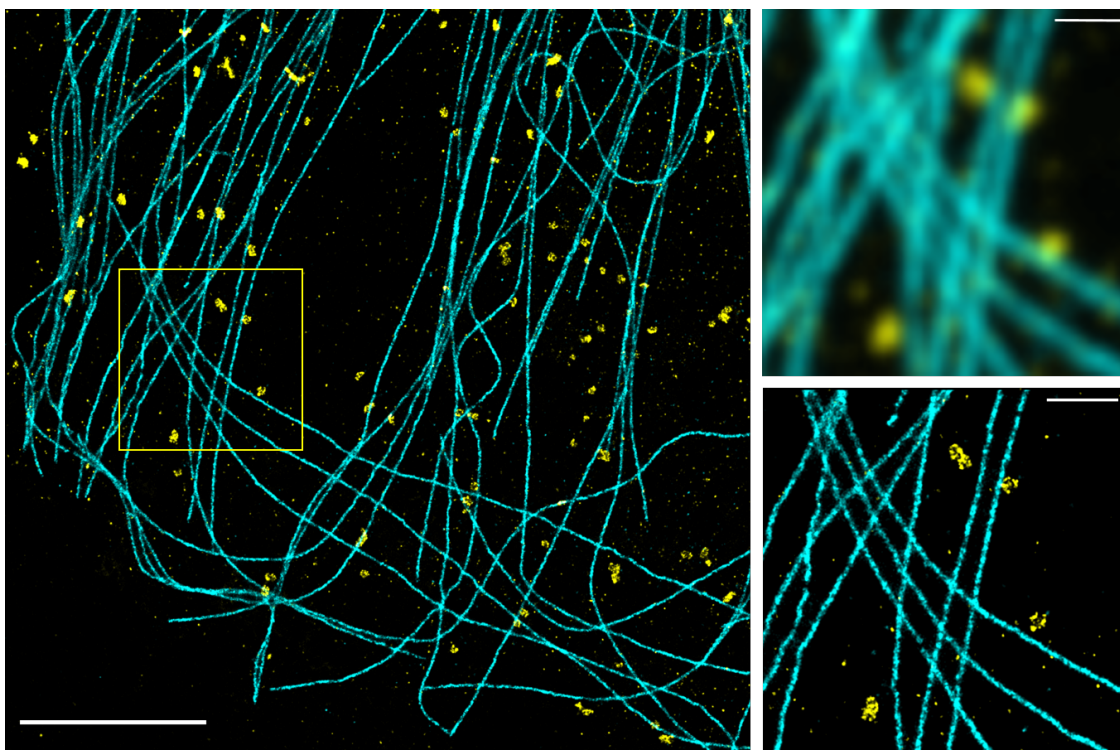


Figure 6: 2-color STORM imaging of microtubules and Clathrin stained with CF-647 and CF-568 respectively. Scalebar: $5\mu m$. Inset: approximated diffraction limited image and STORM image of the region indicated in the yellow box. Scalebar: $1\mu m$ [FRC resolution: 12 nm (CF-568) and 22 nm (CF-647).]

3-color imaging

Finally, we decided to test 3-color imaging, so we stained the cytoskeleton of our COS-7 cells: α -tubulin with CF-750, Clathrin with CF-568 and Actin with Alexa-647 (see Methods). We once

again performed sequential imaging, starting with the reddest fluorophore, and used the 561 nm laser to image CF-568, the increased field of view resulting in a lower intensity ($< 1\text{ kW}/\text{cm}^2$) at this wavelength. Figure 7 shows that this combination works well for multicolor imaging, with minimum cross-talk, good localization precision and good density for all three fluorophores though CF-750 has lower photon counts than the other two dyes. We also tested a few more fluorophores, some of which performed well enough to reconstruct a STORM image (see Table S2 and Figure S12). In particular, Alexa-532 and CF-680 worked in our buffer, which means spectral unmixing^{8,11,12} should be an option to increase the number of colors to 5 for example by sequentially imaging Dy-755, then CF-647 and CF-680, and finally Alexa-532 and CF-568.

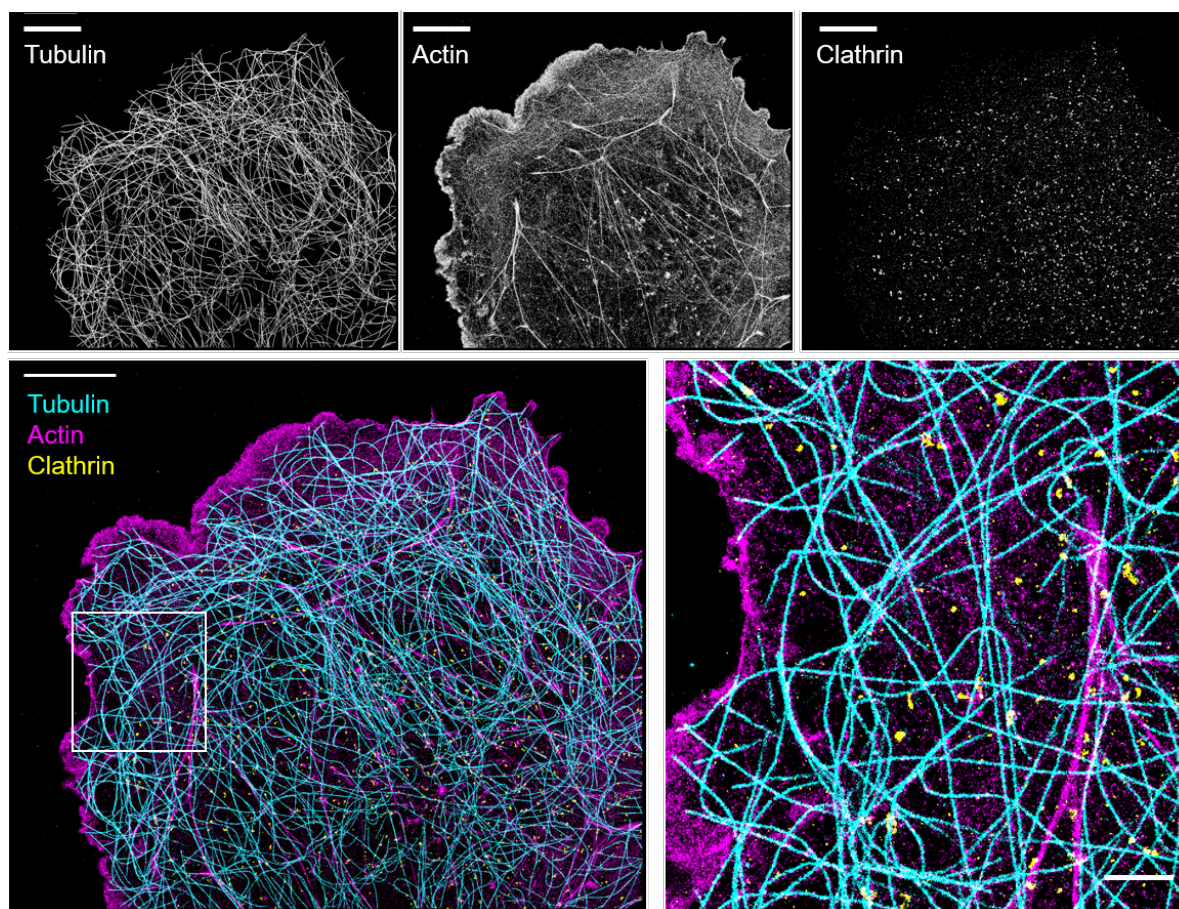


Figure 7: 3-color STORM imaging. Top: From left to right: α -Tubulin (CF-750), Actin (Alexa-647), & Clathrin (CF-568). Bottom: composite image, with α -Tubulin in cyan, actin in magenta and Clathrin in yellow. Scalebar= $10\ \mu\text{m}$, $2\ \mu\text{m}$ in inset. [FRC resolution: 20 nm (CF-568), 29 nm (Alexa-647) and 58 nm (CF-750)].

Conclusions

We have shown that our buffer optimized using a simple microscope, simple sample preparation and simple image analysis allows 3-color STORM imaging using multiple fluorophore combinations, and in particular that it enables high quality 2-color imaging using Alexa-647 and CF-568 (using both 561 nm and 532 nm excitation). This buffer is stable for more than a week, can be frozen and stored at -20°C , and is relatively inexpensive to make. We do not claim that the buffer we presented is better than other buffers, and for 2-color imaging for example the combination of Alexa-647 (or Dylight-649, or CF-647) and CF-750 or Dylight-755 with an optimized buffer^{9,10} is probably preferable. We determined the recipe for our buffer using a fairly simple optimization scheme, with only 4 parameters (concentration of 3 chemicals plus pH) on a single fluorophore, so we expect that further improvements are possible. For example repeating our measurements on 640 nm and 750 nm-excited fluorophores might yield a better 3-color buffer. Our protocol also appears particularly well-suited for STORM imaging of large sample with light-sheet illumination that requires large amounts of buffers. Maybe more importantly, we believe that this stable buffer provides a very good starting point for further optimization, for example by replacing/adding another reducing agent like MEA³⁶ or TCEP,^{9,37} or adding other chemicals such as Propyl Gallate^{16,17} Ascorbic Acid,⁵ or Trolox.³⁸ Indeed, adding COT²⁰ to our buffer and imaging CF-750 yielded an increase in the brightness of the molecule consistent with previous reports (See Figure S11). We quantified the blinking properties of the different dyes tested in our buffer (Figures S4-S10), but did not investigate the photophysical mechanisms behind the blinking we observed.^{6,39,40} Understanding these mechanisms should allow us to further optimize the buffer composition in a more rational manner.

A similar optimization was recently used to improve low-power single-color STORM with Alexa-647,¹⁸ so we expect a broad family of buffers optimized for specific situations to be developed. In particular, optimizing STORM imaging using only low-toxicity ingredients or without salts could be very useful. This approach, in conjunction with the development of new fluorescent dyes optimized for STORM⁴¹ should lead to further improvements for multicolor imaging.

Data availability

- The raw STORM data for the main text and supplemental data are available on Zenodo⁴²
- The FIJI macro used to convert the raw data into STORM images is on github,³⁰ along with the Python code used to quantify photon counts, SNR and density.

Author Contributions

CF-568 buffer optimization: V.A. prepared the samples, performed STORM imaging and analyzed the data. Multicolor imaging: N.O. prepared the samples, V.A. and N.O. performed STORM imaging and V.A. analyzed the data. H.B. performed preliminary experiments and helped set the parameters for the optimization. V.A. and N.O. wrote the article. N.O. supervised the project.

Funding Sources

N.O. acknowledges funding from CNRS (Tremplin@INP 2019 and Tremplin@INP 2021).

Supporting Information Available

Supporting Information Available:

- Supporting Discussion on oxygen scavenging strategies and pH stability.
- Figure S1: Description of the optical setup used for the buffer optimization.
- Figure S2: Quantification of the additional buffers tested.
- Figure S3: FRC maps and FRC resolution of the images from Figure 4-5.
- Figure S4: Further quantification of the blinking of CF-568 in our buffer.
- Figure S5: Further quantification of the blinking of Alexa-647 in our buffer.
- Figure S6: Further quantification of the blinking of Dylight-649 in our buffer.

- Figure S7: Further quantification of the blinking of CF-647 in our buffer.
- Figure S8: Further quantification of the blinking of Cf-750 in our buffer.
- Figure S9: Further quantification of the blinking of Dylight-755 in our buffer.
- Figure S10: Further quantification of the blinking of CF-770 in our buffer.
- Figure S11: STORM imaging of CF-750 with the optimized buffer plus 2 mM COT.
- Figure S12: STORM images of the other fluorophores tested successfully.
- Table S1: Composition of all the buffers used during the optimization.
- Table S2: List of the other dyes tested in the optimized buffer.

This material is available free of charge via the Internet at <http://pubs.acs.org>

Acknowledgement

We thank Sandrine Leveque-Fort for the COS-7 cells and Maxime Mauviel for his help with cell culture, abbelight for the the gift of Clathrin secondary antibody, Nicolas David for Alexa-647 Phalloidin, Beatrice Durel for the Alexa-532 and Cy3 antibodies, Vectorlab for the gift of the Dylight-649 antibody, Biotium for the gift of CF-532, CF-660C and CF-770 secondary antibodies. We thank Debora Keller-Olivier, Kate Sorg, and Dorian Noury for critical reading, and all the members of the "nano" group at LOB for scientific and technical discussions.

References

- (1) Rust, M. J.; Bates, M.; Zhuang, X. Sub-diffraction-limit imaging by stochastic optical reconstruction microscopy (STORM). *Nature methods* **2006**, *3*, 793–796.

- (2) Dasgupta, A.; Deschamps, J.; Matti, U.; Hübner, U.; Becker, J.; Strauss, S.; Jungmann, R.; Heintzmann, R.; Ries, J. Direct supercritical angle localization microscopy for nanometer 3D superresolution. *Nature communications* **2021**, *12*, 1–9.
- (3) Bates, M.; Blosser, T. R.; Zhuang, X. Short-range spectroscopic ruler based on a single-molecule optical switch. *Physical review letters* **2005**, *94*, 108101.
- (4) Heilemann, M.; Margeat, E.; Kasper, R.; Sauer, M.; Tinnefeld, P. Carbocyanine dyes as efficient reversible single-molecule optical switch. *Journal of the American Chemical Society* **2005**, *127*, 3801–3806.
- (5) Steinhauer, C.; Forthmann, C.; Vogelsang, J.; Tinnefeld, P. Superresolution microscopy on the basis of engineered dark states. *Journal of the American Chemical Society* **2008**, *130*, 16840–16841.
- (6) Dempsey, G. T.; Bates, M.; Kowtoniuk, W. E.; Liu, D. R.; Tsien, R. Y.; Zhuang, X. Photo-switching mechanism of cyanine dyes. *Journal of the American Chemical Society* **2009**, *131*, 18192–18193.
- (7) Dempsey, G. T.; Vaughan, J. C.; Chen, K. H.; Bates, M.; Zhuang, X. Evaluation of fluorophores for optimal performance in localization-based super-resolution imaging. *Nature methods* **2011**, *8*, 1027.
- (8) Lehmann, M.; Lichtner, G.; Klenz, H.; Schmoranzler, J. Novel organic dyes for multicolor localization-based super-resolution microscopy. *Journal of biophotonics* **2016**, *9*, 161–170.
- (9) Zhao, T.; Wang, Y.; Zhai, Y.; Qu, X.; Cheng, A.; Du, S.; Loy, M. A user-friendly two-color super-resolution localization microscope. *Optics express* **2015**, *23*, 1879–1887.
- (10) Douglass, K. M.; Sieben, C.; Archetti, A.; Lambert, A.; Manley, S. Super-resolution imaging of multiple cells by optimized flat-field epi-illumination. *Nature photonics* **2016**, *10*, 705–708.

- (11) Winterflood, C. M.; Platonova, E.; Albrecht, D.; Ewers, H. Dual-color 3D superresolution microscopy by combined spectral-demixing and biplane imaging. *Biophysical journal* **2015**, *109*, 3–6.
- (12) Platonova, E.; Winterflood, C. M.; Ewers, H. A simple method for GFP-and RFP-based dual color single-molecule localization microscopy. *ACS chemical biology* **2015**, *10*, 1411–1416.
- (13) Andronov, L.; Genthial, R.; Hentsch, D.; Klaholz, B. P. splitSMLM, a spectral demixing method for high-precision multi-color localization microscopy applied to nuclear pore complexes. *Communications biology* **2022**, *5*, 1–13.
- (14) Ries, J. SMAP: a modular super-resolution microscopy analysis platform for SMLM data. *Nature Methods* **2020**, *17*, 870–872.
- (15) Hartwich, T. M.; Chung, K. K. H.; Schroeder, L.; Bewersdorf, J.; Soeller, C.; Baddeley, D. A stable, high refractive index, switching buffer for super-resolution imaging (November 08, 2018.). *bioRxiv*. <https://www.biorxiv.org/content/10.1101/465492v1> (accessed 2022-10-26).
- (16) Johnson, G.; Davidson, R.; McNamee, K.; Russell, G.; Goodwin, D.; Holborow, E. Fading of immunofluorescence during microscopy: a study of the phenomenon and its remedy. *Journal of immunological methods* **1982**, *55*, 231–242.
- (17) Olivier, N.; Keller, D.; Rajan, V. S.; Gönczy, P.; Manley, S. Simple buffers for 3D STORM microscopy. *Biomedical optics express* **2013**, *4*, 885–899.
- (18) Chung, J.; Jeong, U.; Jeong, D.; Go, S.; Kim, D. Development of a New Approach for Low-Laser-Power Super-Resolution Fluorescence Imaging. *Analytical Chemistry* **2021**, *94*, 618–627.
- (19) Swoboda, M.; Henig, J.; Cheng, H.-M.; Brugger, D.; Haltrich, D.; Plumeré, N.; Schlierf, M.

- Enzymatic oxygen scavenging for photostability without pH drop in single-molecule experiments. *ACS nano* **2012**, *6*, 6364–6369.
- (20) Olivier, N.; Keller, D.; Gönczy, P.; Manley, S. Resolution doubling in 3D-STORM imaging through improved buffers. *PloS one* **2013**, *8*, e69004.
- (21) Herdly, L.; Tinning, P. W.; Geiser, A.; Taylor, H.; Gould, G. W.; van de Linde, S. Benchmarking thiolate driven photoswitching of cyanine dyes (September 15, 2022). *bioRxiv*. <https://www.biorxiv.org/content/10.1101/2022.09.15.507984v1> (accessed 2022-10-26).
- (22) Huang, B.; Jones, S. A.; Brandenburg, B.; Zhuang, X. Whole-cell 3D STORM reveals interactions between cellular structures with nanometer-scale resolution. *Nature methods* **2008**, *5*, 1047–1052.
- (23) Tokunaga, M.; Imamoto, N.; Sakata-Sogawa, K. Highly inclined thin illumination enables clear single-molecule imaging in cells. *Nature methods* **2008**, *5*, 159–161.
- (24) Martens, K. J.; van Beljouw, S. P.; van der Els, S.; Vink, J. N.; Baas, S.; Vogelaar, G. A.; Brouns, S. J.; van Baarlen, P.; Kleerebezem, M.; Hohlbein, J. Visualisation of dCas9 target search in vivo using an open-microscopy framework. *Nature communications* **2019**, *10*, 1–11.
- (25) Diekmann, R.; Kahnwald, M.; Schoenit, A.; Deschamps, J.; Matti, U.; Ries, J. Optimizing imaging speed and excitation intensity for single-molecule localization microscopy. *Nature methods* **2020**, *17*, 909–912.
- (26) Jimenez, A.; Friedl, K.; Leterrier, C. About samples, giving examples: optimized single molecule localization microscopy. *Methods* **2020**, *174*, 100–114.
- (27) Edelstein, A. D.; Tsuchida, M. A.; Amodaj, N.; Pinkard, H.; Vale, R. D.; Stuurman, N. Advanced methods of microscope control using μ Manager software. *Journal of biological methods* **2014**, *1*, No. e10.

- (28) Chazeau, A.; Katrukha, E. A.; Hoogenraad, C. C.; Kapitein, L. C. *Methods in Cell Biology*; Elsevier, 2016; Vol. 131; pp 127–149.
- (29) Martens, K. J.; Bader, A. N.; Baas, S.; Rieger, B.; Hohlbein, J. Phasor based single-molecule localization microscopy in 3D (pSMLM-3D): An algorithm for MHz localization rates using standard CPUs. *The Journal of chemical physics* **2018**, *148*, 123311.
- (30) Abdelsayed, V.; Boukathem, H.; Olivier, N. GitHub. https://github.com/LaboratoryOpticsBiosciences/STORM_Analysis (accessed 2022-10-27).
- (31) Nieuwenhuizen, R. P.; Lidke, K. A.; Bates, M.; Puig, D. L.; Grünwald, D.; Stallinga, S.; Rieger, B. Measuring image resolution in optical nanoscopy. *Nature methods* **2013**, *10*, 557–562.
- (32) Herbert, A.; Burri, O. GitHub. <https://github.com/BIOP/ijp-frc> (accessed 2022-10-27).
- (33) Letterier, C. GitHub. <https://github.com/cleterrier/ChriSTORM> (accessed 2022-10-27).
- (34) Leterrier, C.; Potier, J.; Caillol, G.; Debarnot, C.; Boroni, F. R.; Dargent, B. Nanoscale architecture of the axon initial segment reveals an organized and robust scaffold. *Cell reports* **2015**, *13*, 2781–2793.
- (35) Bates, M.; Huang, B.; Dempsey, G. T.; Zhuang, X. Multicolor super-resolution imaging with photo-switchable fluorescent probes. *Science* **2007**, *317*, 1749–1753.
- (36) Heilemann, M.; Van De Linde, S.; Schüttelpelz, M.; Kasper, R.; Seefeldt, B.; Mukherjee, A.; Tinnefeld, P.; Sauer, M. Subdiffraction-resolution fluorescence imaging with conventional fluorescent probes. *Angewandte Chemie International Edition* **2008**, *47*, 6172–6176.
- (37) Vaughan, J. C.; Dempsey, G. T.; Sun, E.; Zhuang, X. Phosphine quenching of cyanine dyes

- as a versatile tool for fluorescence microscopy. *Journal of the American Chemical Society* **2013**, *135*, 1197–1200.
- (38) Rasnik, I.; McKinney, S. A.; Ha, T. Nonblinking and long-lasting single-molecule fluorescence imaging. *Nature methods* **2006**, *3*, 891–893.
- (39) Ha, T.; Tinnefeld, P. Photophysics of fluorescent probes for single-molecule biophysics and super-resolution imaging. *Annual review of physical chemistry* **2012**, *63*, 595–617.
- (40) Levitus, M. *Spectroscopy and Dynamics of Single Molecules*; Elsevier, 2019; pp 15–69.
- (41) Wang, B.; Xiong, M.; Susanto, J.; Li, X.; Leung, W.-Y.; Xu, K. Transforming Rhodamine Dyes for (d) STORM Super-Resolution Microscopy via 1, 3-Disubstituted Imidazolium Substitution. *Angewandte Chemie* **2022**, *134*, e202113612.
- (42) Abdelsayed, V.; Boukathem, H.; Olivier, N. Zenodo. <https://doi.org/10.5281/zenodo.7252469> (accessed 2022-10-27).

TOC Graphic

